

VII. ÖRÆFAJÖKULL: EVACUATION TIME MODELLING OF AREAS PRONE TO VOLCANOGENIC FLOODS

Emmanuel Pagneux *

* *Icelandic Meteorological Office*

1. Introduction

In this study, modelling of the time available at eruption onset and of the time required for a full evacuation of areas exposed to floods due to eruptive activity of Öräfajökull Volcano is realised and evacuation routes identified.

The aim of the study is to provide the authorities in charge of the emergency response — primarily the Department of Civil Protection and Emergency Management of the National Commissioner of the Icelandic Police and the local authorities — with baseline figures for the development of an effective flood evacuation plan. When evacuation should be ordered and to which extent it should be done are key considerations laying in the background of the study. It is likely that any eruption of the volcano will be foreseen days in advance. Using seismic stations, the imminence of a volcanic eruption can be fairly approached through the detection of changes in the rate of occurrence of volcano-tectonic earthquakes and the formation of harmonic tremor, considered both seismic precursors of volcanic activity (Zobin, 2011). Assuming that eruption onset will be clearly and immediately established through detection of volcanic tremor (e.g. Vogfjörd *et al.*, 2005), the main question of interest for the emergency response is of the time available and of the time required for evacuation upon signal detection. It may be mentioned that hesitation of the authorities to

order an early evacuation of the Colombian cities of Armero and Chinchina during the 1985 Nevado Del Ruiz eruption resulted in the deaths of 25,000 individuals, buried in the body of high-velocity lahars (Voight, 1990; Mileti *et al.*, 1991).

1.1. Study area

Öräfajökull is an ice-capped stratovolcano located in south-east Iceland that dominates and threatens the Öräfi district (Figure VII-1). The district is delimited to the West by the Skeiðará river and to the East by the Fjallsá river (Figure VII-2).

The volcano erupted on two occasions in historical times. The first known historical eruption occurred in 1362 CE. The eruption was highly explosive, reaching VEI 6 (Gudmundsson *et al.*, 2008), and caused massive floods on the western slopes of the volcano and in the adjacent lowland (Thorarinsson, 1958; Roberts and Gudmundsson, 2015). The ash fall and floods together resulted in the death of ~300 individuals (Thorarinsson, 1958). Following the 1362 CE eruption, the Öräfi district remained mostly uninhabited for centuries, which probably explains that the second eruption, in 1727 CE, resulted in only three fatalities, although causing floods of magnitude comparable to those of 1362 CE (Thorarinsson, 1958; Roberts and Gudmundsson, 2015).

The Öräfi district now hosts the main service centre of the Vatnajökull National Park and attracts thousands of tourists during the summer seasonal high. Estimations on night-time exposure (Pagneux, 2015) suggest a maximum of ~830 individuals staying overnight in the district, thereof 130 in the area identified at risk of flooding in the hydraulic simulations performed by Helgadóttir *et al.* (2015) and 240 in areas potentially isolated by the simulated floods.

The hydraulic simulations performed by Helgadóttir *et al.* (2015) build upon melting scenarios elaborated by Gudmundsson *et al.* (2015). Three sources of melting were considered in the scenarios: eruption in the caldera, eruptions on the flanks of the volcano, and the formation of pyroclastic density currents (PDC). The numerical simulations were performed as instant release waves flowing at the surface of the glacier using 0.05 and 0.10 $\text{sm}^{-1/3}$ average Manning roughness coefficients. Results on the extent of floods suggest that 347 km^2 of land are at risk of flooding, thereof 284 km^2 exposed to floods

caused by a caldera eruption, flank eruptions, or pyroclastic density currents (Figure VII-2), 42 km^2 to floods caused by flank eruptions or pyroclastic density currents, and 21 km^2 to floods caused by pyroclastic density currents only. From the lower boundary of the release areas down to the National road, the minimum flood travel times found ranged 6 – 21 minutes.

Using thresholds in computed depths of flooding and flow velocities on one hand, considering the presence of life-threatening debris and temperature of floodwater on the other, Pagneux and Roberts (2015) have proposed to rate flood hazards in the area identified at risk of flooding as high or extreme exclusively. High hazard means that all lives are in jeopardy, outside and inside inhabited buildings. Extreme hazard means that jökulhlaups have the potential to destroy completely non-reinforced buildings and cause damage to reinforced concrete dwellings to a degree that would require demolition in the recovery phase.

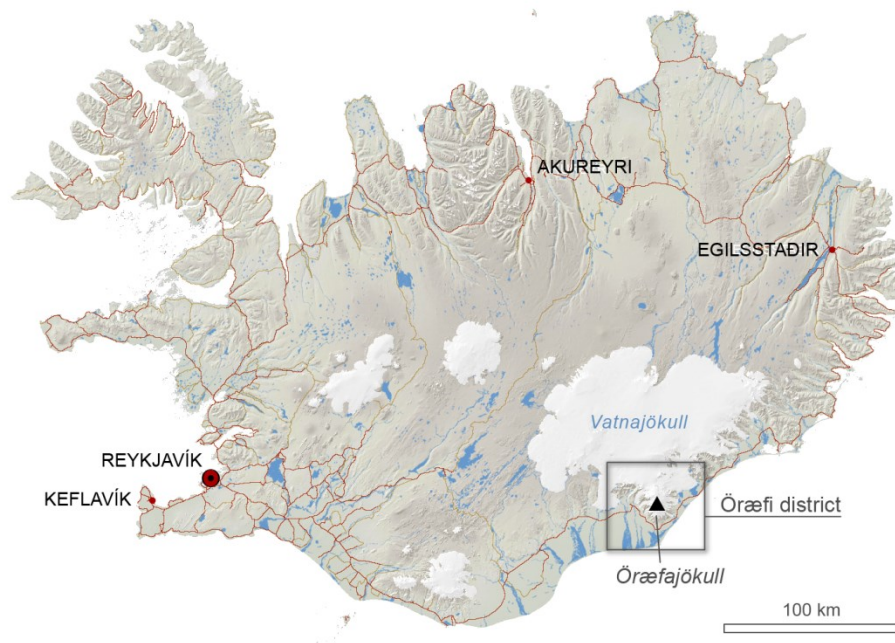


Figure VII-1: Location of the Öräfajökull ice-capped stratovolcano.

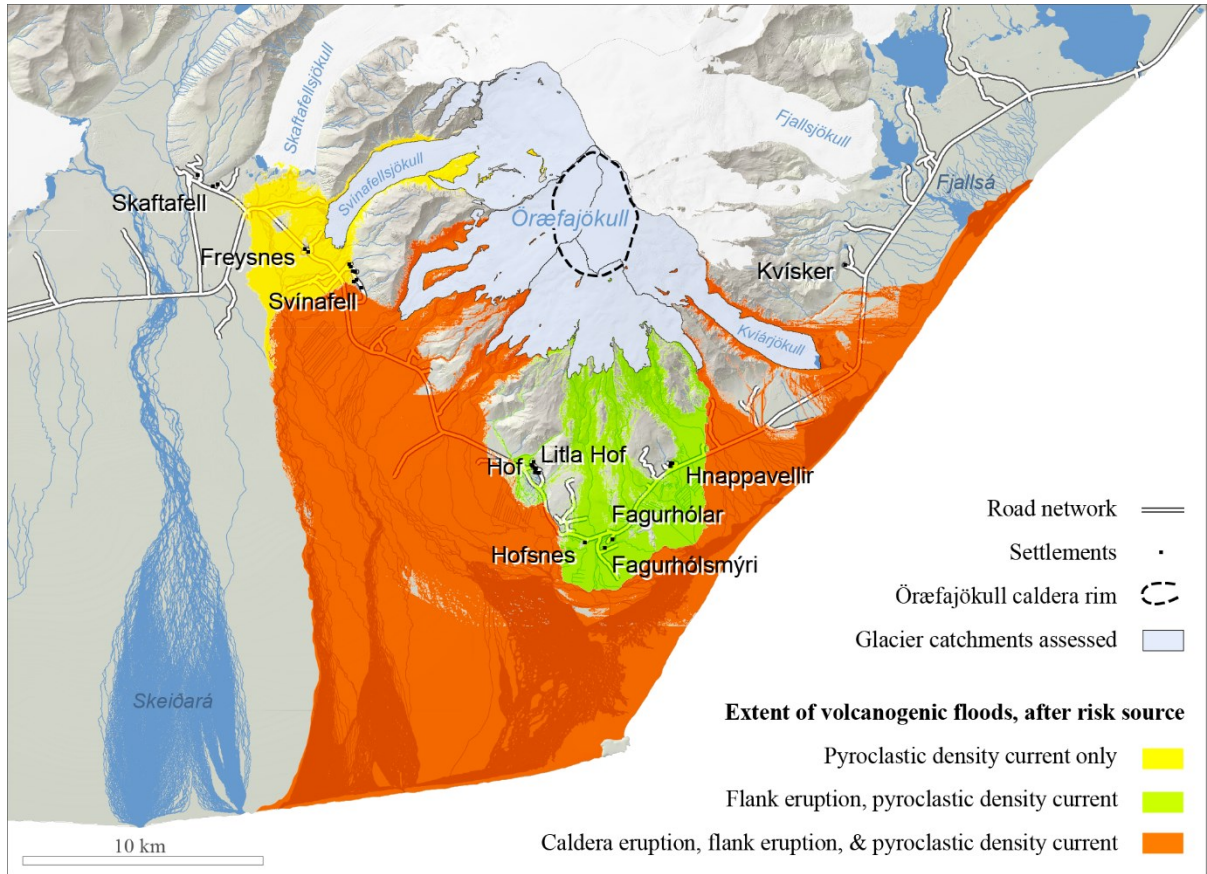


Figure VII-2: Inundation extent of scenario-based floods caused by volcanic activity of Öraefajökull volcano. Taken from Helgadóttir *et al.*, 2015.

2. Available time for evacuation

In this study, the time available until the National road gets flooded was used as an expression of the time available for evacuation.

Estimations were made at the onset of volcanic eruptions initiated in the caldera or on the flanks of the volcano, as well as at onset of pyroclastic density currents. The melting scenarios proposed by Gudmundsson *et al.* (2015), and the results of the numerical simulations performed accordingly by Helgadóttir *et al.* (2015) were used for the estimations.

Available time in the case of floods caused by a caldera eruption (AT_{ce}) was estimated as the sum of minimum eruption onset time (EOT_{min}), minimum subglacial flood transport time ($SbTT_{min}$), and minimum

transport times at onset of supraglacial flows on the volcano flanks ($SpTT_{min}$):

$$AT_{ce} = EOT_{min} + SbTT_{min} + SpTT_{min}$$

Available time in the case of floods caused by flank eruptions (AT_{fe}) was estimated as the sum of minimum eruption onset time (EOT_{min}) and minimum transport times at onset of supraglacial flows ($SpTT_{min}$):

$$AT_{fe} = EOT_{min} + SpTT_{min}$$

Available time in the case of floods caused by the formation of pyroclastic density currents (AT_{pdc}) was estimated as the sum of minimum PDC onset time (POT_{min}) and minimum transport times at onset of supraglacial flows ($SpTT_{min}$):

$$AT_{pdc} = POT_{min} + SpTT_{min}$$

The minimum subglacial flood transport time expresses the minimum time that floodwater spends migrating under the ice, on its way from the caldera eruption site to the point, on the glaciated slopes of the volcano, where the outburst is expected to turn from a pure subglacial event into a dominant supraglacial flood (Figure VII-3), and therefore does not account for the possible retention of melting water in the caldera before flood release.

The use of subglacial flow transport time was not required for the estimation of the time available for evacuation in scenarios where floods are caused by flank eruptions and the formation of pyroclastic density currents, as meltwater has its origin at the glacier's surface (Figure VII-3).

The time available at onset of the supraglacial flows ($SpTT_{min}$) was determined using the minimum surface transport times estimated by Helgadóttir *et al.* (2015) at predefined peak discharge ($SrTT_{Q_{max}}$) along with estimations of:

- i. The time elapsed from the onset of supraglacial flows until the maximum discharge is reached ($t_{Q_{max}}$);
- ii. The transport times at intermediate discharge ($SrTT_{Q_1}$);

- iii. The time elapsed from the onset of floods until intermediary discharge (t_{Q_1}) is reached.

When $SrTT_{Q_1}$ was known or could be inferred, the minimum time effectively available at onset of any supraglacial flow was defined as

$$SpTT_{min} = \min\{SpTT_{Q_1}; SpTT_{Q_{max}}\},$$

$$\text{where } SpTT_{Q_1} = SrTT_{Q_1} + t_{Q_1} \text{ and}$$

$$SpTT_{Q_{max}} = SrTT_{Q_{max}} + t_{Q_{max}}$$

When $SrTT_{Q_1}$ could not be estimated, definition of the minimum time effectively available at onset of supraglacial flows was reduced to

$$SpTT_{min} = SpTT_{Q_{max}}$$

For each risk source (caldera eruption, flank eruption and PDC formation), the value of t_Q was determined using rising rates in the form of $Q = xt$ (where Q is discharge and t the time from onset of supraglacial flow).

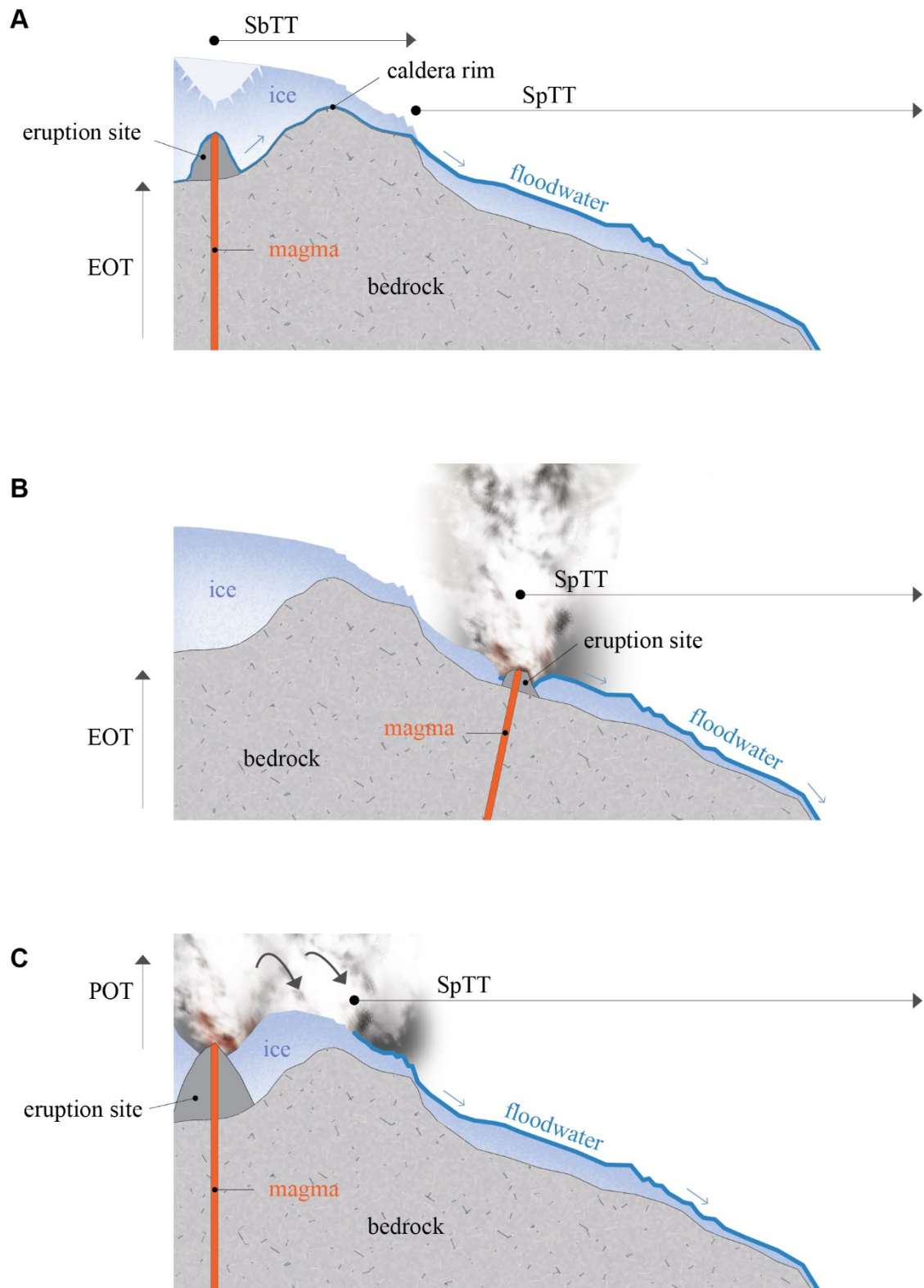


Figure VII-3: Schematic representation of the time sequences defining the time available for evacuation in the case of jökulhlaups caused by a caldera eruption (A), flank eruptions (B), and the formation of pyroclastic density currents (C). EOT: Eruption onset time; SbTT: Subglacial flow transport time; SpTT: transport time at onset of supraglacial flow; POT: Onset time of pyroclastic density current.

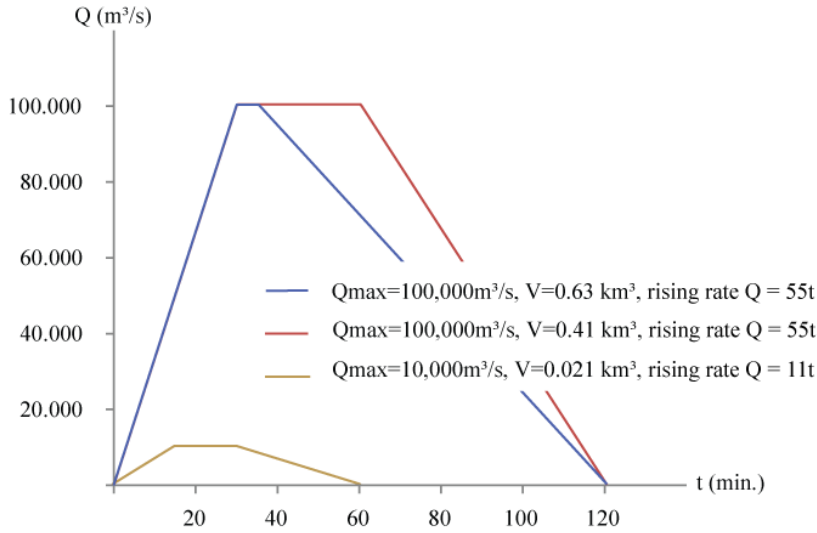


Figure VII-4: Plausible hydrographs for jökulhlaups caused by an eruption of Öraefajökull Volcano (After Gudmundsson *et al.*, 2015). Rising rate in the concentration phase is approximated as $Q = 55t$ for catastrophic floods and $Q = 11t$ for moderate floods (Where Q is discharge and t the time from onset of supraglacial flow).

2.1. At onset of a caldera eruption

2.1.1. Eruption onset time and subglacial transport time

Gudmundsson *et al.* (2015) suggest for a caldera eruption minimum eruption onset time and minimum subglacial flood transport time of 15 and five minutes, respectively.

2.1.2. Available time at onset of supraglacial flow

There is little evidence to support the choice of a particular rising rate. Using inferences from Alaska and Iceland, Gudmundsson *et al.* (2015) suggest for catastrophic floods caused by caldera eruptions of Öraefajökull Volcano an approximate rising rate in the form of $Q = 55t$ (Figure VII-4). At such a rate, $Q_{max} = 100,000 \text{ m}^3/\text{s}$ is reached within 30 minutes from the onset of the flow at the glacier's surface.

Simulations of supraglacial floodwater released in the Virkisjökull - Falljökull drainage area at discharge $Q_1 = 10,000 \text{ m}^3/\text{s}$ and $Q_{max} = 100,000 \text{ m}^3/\text{s}$ alternatively (Helgadóttir *et al.*, 2015) indicate that surface transport times at discharge Q_1 represent a 2.06 increase of the transport times at discharge Q_{max} :

$$SrTT_{Q_1} = 2.06 \cdot SrTT_{Q_{max}}$$

If we assume, in every glacier catchment assessed, a rising rate $Q = 55t$ and a 2.06 increase factor in transport time between a $10,000 \text{ m}^3/\text{s}$ discharge and a $100,000 \text{ m}^3/\text{s}$ discharge, we find $SpTT_{Q_1}$ to be smaller than $SpTT_{Q_{max}}$ (Table VII-1):

$$\text{If } Q = 55t, SrTT_{Q_1} = 2.06 \cdot SrTT_{Q_{max}}, \text{ and } SpTT_{Q_1} = SrTT_{Q_1} + t_{Q_1}$$

$$\text{therefore } SpTT_{Q_1} < SpTT_{Q_{max}}$$

As a consequence, if the rising rate is in the form of $Q = 55t$, we find $SpTT_{Q_1}$ to be a better approximation of $SpTT_{min}$ than $SpTT_{Q_{max}}$ is:

$$SpTT_{min} = SpTT_{Q_1}$$

Should in turn the maximum discharge be attained at the onset of the supraglacial flows ($t_{Q_{max}} = 0$), $SpTT_{Q_{max}}$ would be the equivalent of $SpTT_{min}$:

$$SpTT_{min} = SpTT_{Q_{max}}$$

Table VII-1: Values of $SpTT_Q$ at discharge $Q_1 = 10,000m^3/s$ and $Q_{max} = 100,000m^3/s$ using as assumptions an increase time ratio $SrTT_{Q_1} = 2.06 \cdot SrTT_{Q_{max}}$ and a rising rate $Q = 55t$.

Glacier catchment	Discharge Q (m ³ /s)	Manning n (sm ^{-1/3})	t_Q (min.)	$SrTT_Q$ (min.)	$SpTT_Q$ (min.)
Falljökull – Virkisjökull	10,000	0.05	3	14	17
		0.1		31	34
	100,000	0.05	30	7	37
		0.1		15	45
Kotárjökull	10,000	0.05	3	12	15
		0.1		27	30
	100,000	0.05	30	6	36
		0.1		13	43
Kvíarjökull	10,000	0.05	3	19	22
		0.1		41	44
	100,000	0.05	30	9	39
		0.1		20	50

Table VII-2: Values of $SpTT_Q$ at discharge $Q_{max} = 100,000m^3/s$, using $t_{Q_{max}} = 0$ as an assumption (peak discharge attained at onset of supraglacial flow).

Glacier catchment	Discharge Q (m ³ /s)	Manning n (sm ^{-1/3})	t_Q (min.)	$SrTT_Q$ (min.)	$SpTT_Q$ (min.)
Falljökull – Virkisjökull	100,000	0.05	0	7	7
		0.1		15	15
Kotárjökull	100,000	0.05	0	6	6
		0.1		13	13
Kvíarjökull	100,000	0.05	0	9	9
		0.1		20	20

2.1.3. Computed evacuation time

Results of the calculations indicate that at onset of a caldera eruption, the minimum time available before the National road gets

flooded is 26 – 29 minutes using $t_{Q_{max}} = 0$ (Figure VII-5, Figure VII-8) and 35 – 42 minutes using rising rate $Q = 55t$ (Figure VII-6, Figure VII-8).

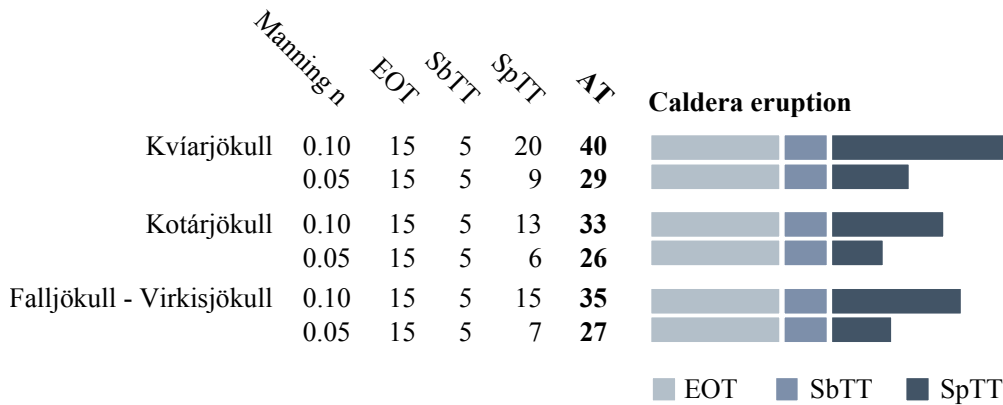


Figure VII-5: Available time at onset of a caldera eruption (AT_{ce}), before floodwater reaches the National road. $AT_{ce} = EOT_{min} + SbTT_{min} + SpTT_{min}$. Maximum discharge attained at onset of supraglacial flow ($t_{Q_{max}} = 0$) is used as an assumption.

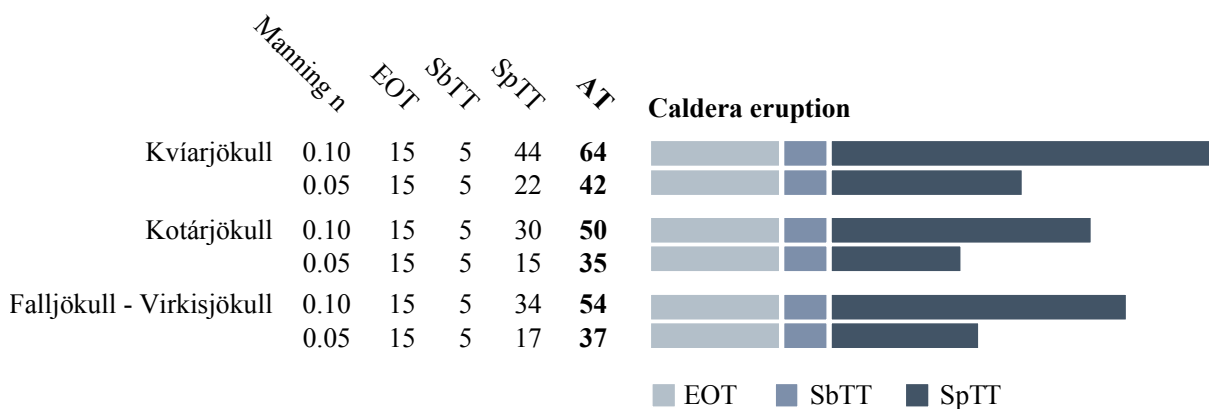


Figure VII-6: Available time at onset of a caldera eruption (AT_{ce}), before floodwater reaches the National road. $AT_{ce} = EOT_{min} + SbTT_{min} + SpTT_{min}$. An increase time ratio $SrTT_{Q_1} = 2.06 \cdot SrTT_{Q_{max}}$ and a rising rate $Q = 55t$ are used as assumptions.

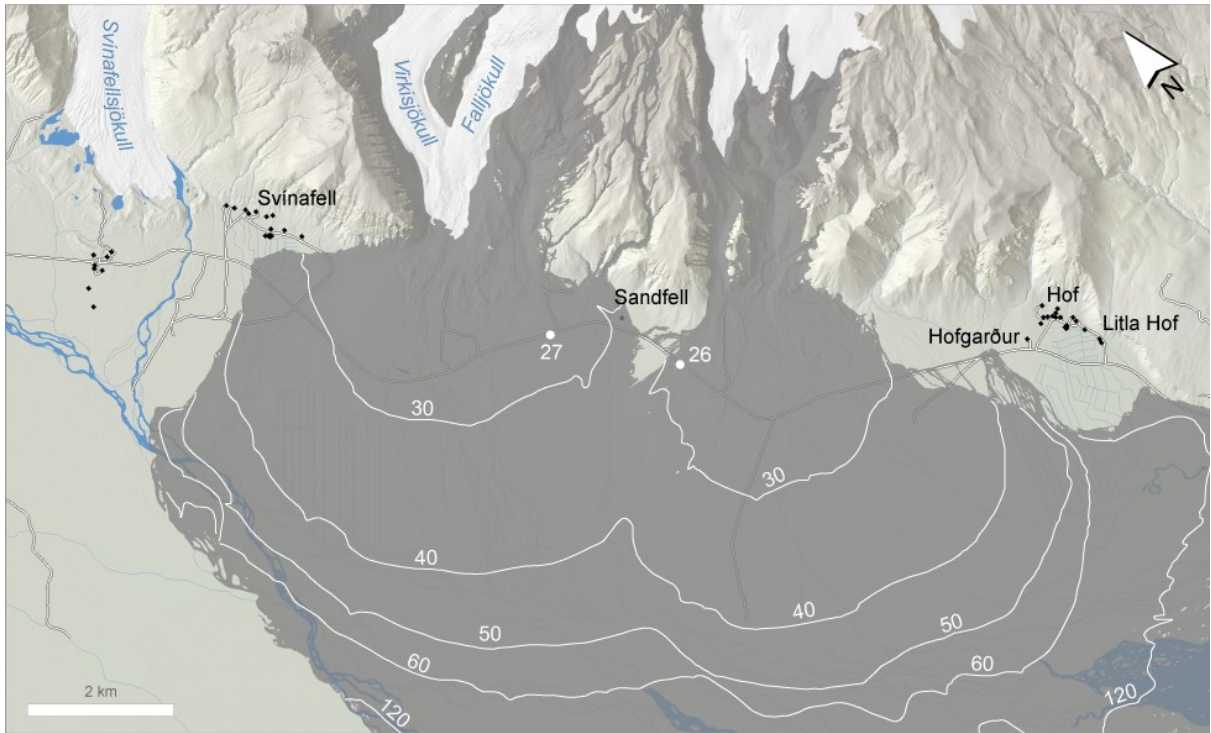


Figure VII-7: Minimum time available for evacuation (10-min isochrones) should a caldera eruption cause floods flowing down in the Falljökull – Virkisjökull and Kotárjökull drainage areas. Maximum discharge attained at onset of supraglacial flow ($t_{Q_{max}} = 0$) is used as an assumption. Inundation extent in the proglacial area is shown as a grey overlay.

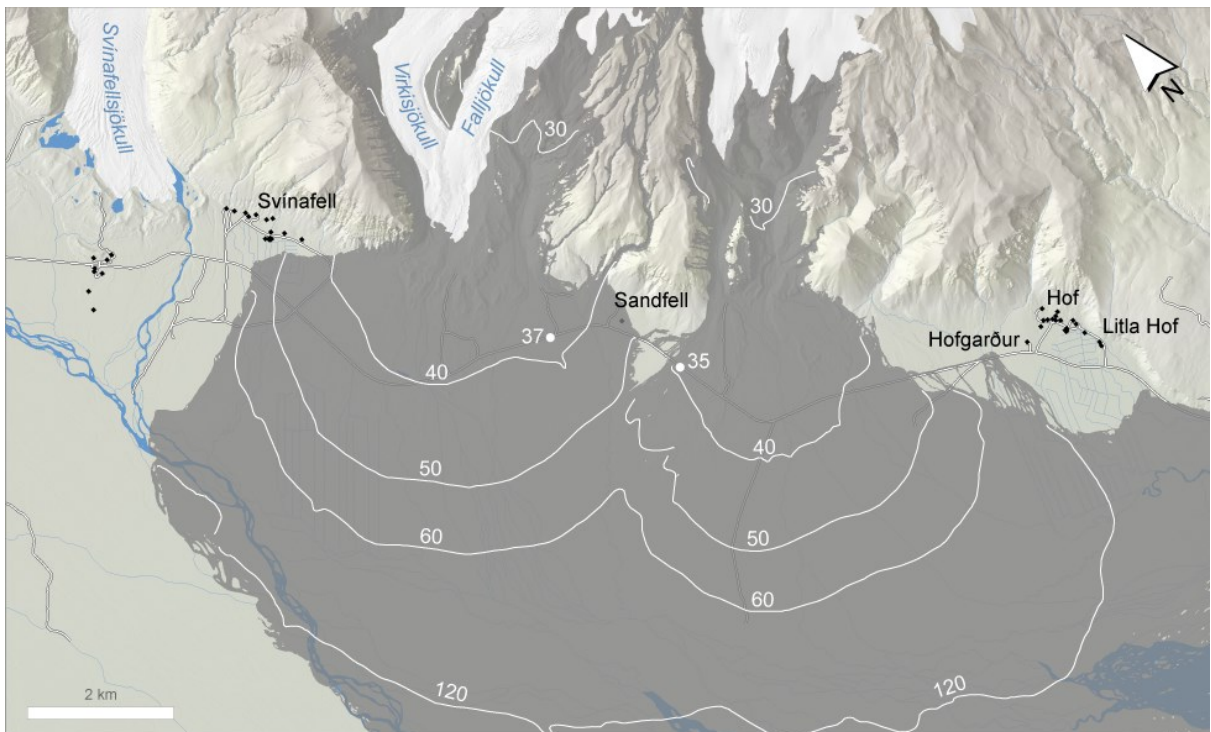


Figure VII-8: Minimum time available for evacuation (10-min isochrones) should a caldera eruption cause floods flowing down in the Falljökull – Virkisjökull and Kotárjökull drainage areas. An increase time ratio $SrTT_{Q_1} = 2.06 \cdot SrTT_{Q_{max}}$ and a rising rate $Q = 55t$ are used as assumptions. Inundation extent in the proglacial area is shown as a grey overlay.

2.2. At onset of flank eruptions

As for an eruption taking place in the caldera, Gudmundsson *et al.* (2015) suggest for flank eruptions a minimum eruption onset time (EOT_{min}) of 15 minutes.

Available time at onset of supraglacial flow was estimated using alternatively $t_{Q_{max}} = 0$ min. and $t_{Q_{max}} = 15$ min. (approximate rising rate $Q = 11t$, see Figure VII-4).

As a comparison between $SpTT_{Q_{max}}$ and $SpTT_{Q_1}$ could not be performed, $SpTT_{Q_{max}}$ was considered the equivalent of $SpTT_{min}$ when $Q = 11t$ was used.

Results of the calculations indicate that at onset of a flank eruption, the minimum time available before the National road gets flooded is 19 – 32 minutes using $t_{Q_{max}} = 0$ (Figure VII-9, Figure VII-11) and 34 – 47 minutes using rising rate $Q = 11t$ (Figure VII-10, Figure VII-12).

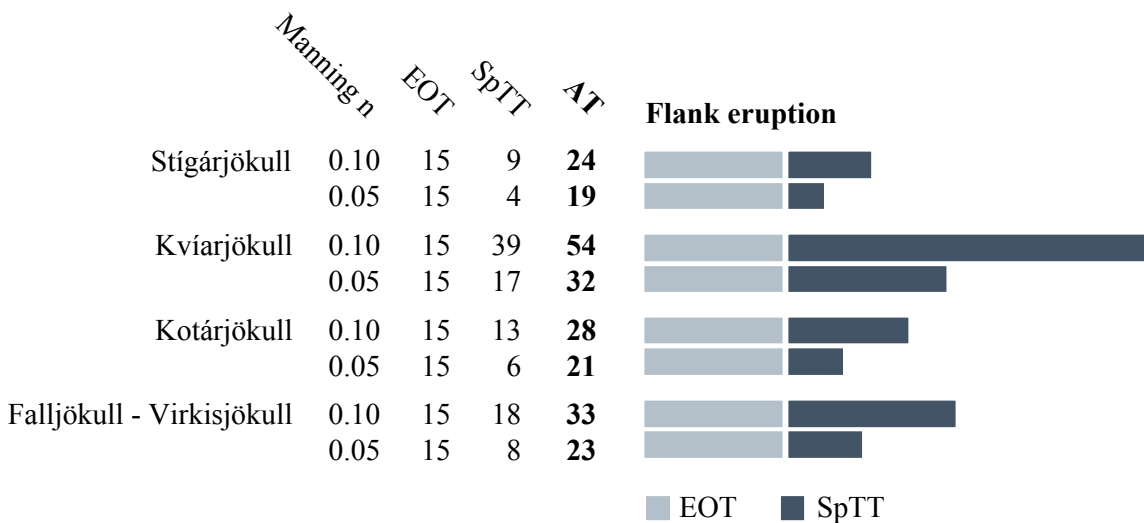


Figure VII-9: Available time at onset of a flank eruption (AT_{fe}) before floodwater reaches the National road. $AT_{fe} = EOT_{min} + SpTT_{min}$. Maximum discharge attained at onset of supraglacial flow ($t_{Q_{max}} = 0$) is used as an assumption.

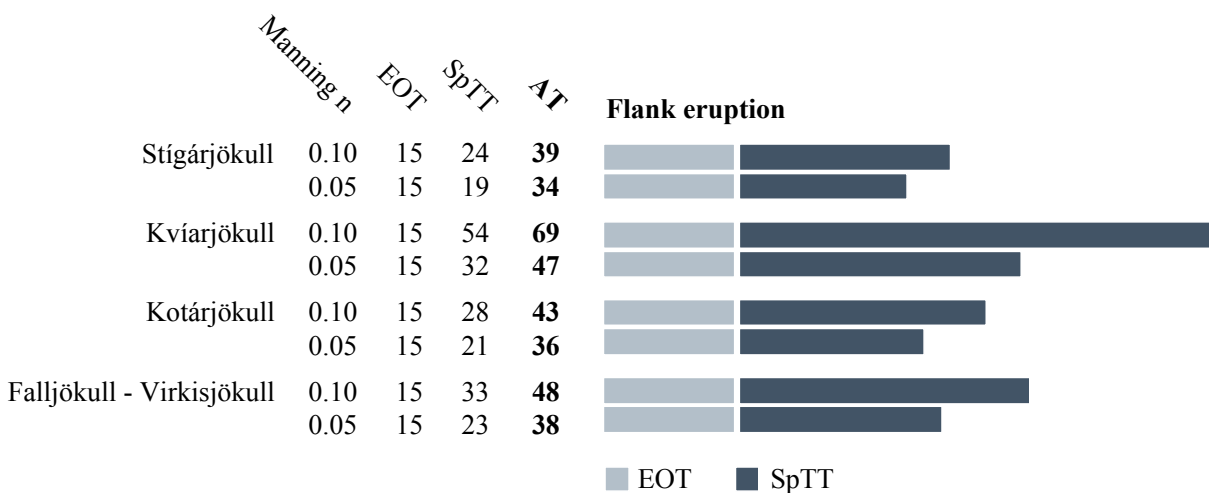


Figure VII-10: Available time at onset of a flank eruption (AT_{fe}) before floodwater reaches the National road. $AT_{fe} = EOT_{min} + SpTT_{min}$. A rising rate $Q = 11t$ is used as an assumption.

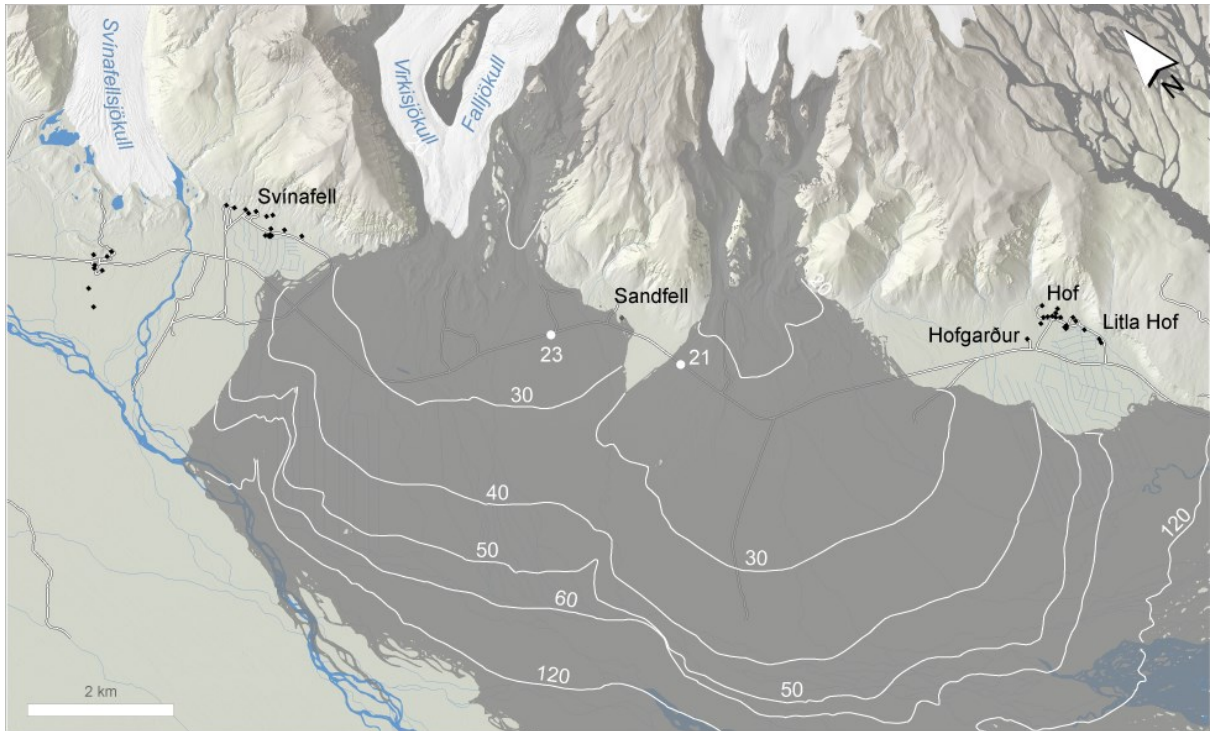


Figure VII-11: Minimum time available for evacuation (10-min isochrones) should a flank eruption cause floods in the Falljökull – Virkisjökull and Kotárjökull drainage areas. Maximum discharge attained at onset of supraglacial flow ($t_{Q_{max}} = 0$) is used as an assumption. Inundation extent in the proglacial area is shown as a grey overlay.

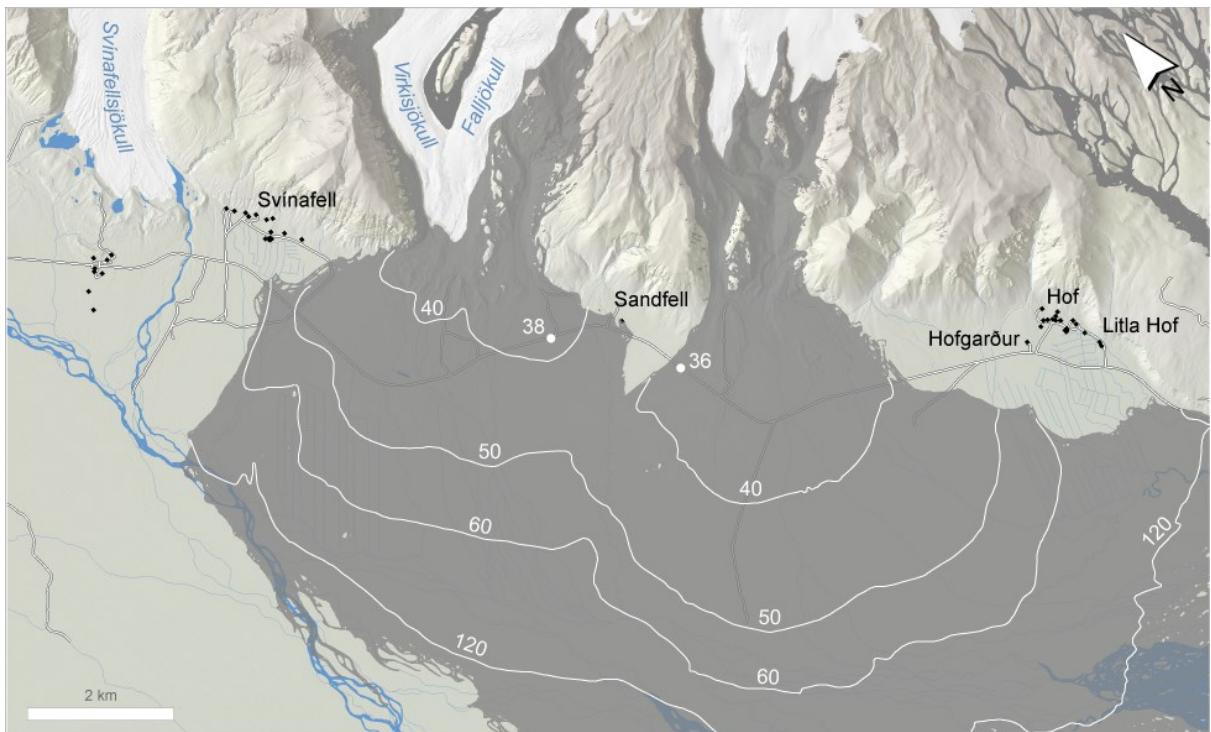


Figure VII-12: Minimum time available for evacuation (10-min isochrones) should a flank eruption cause floods in the Falljökull – Virkisjökull and Kotárjökull drainage areas. Rising rate $Q = 11t$ is used as an assumption. Inundation extent in the proglacial area is shown as a grey overlay.

2.3. At onset of pyroclastic density currents

The value of POT_{min} was fixed to 5 minutes (Gudmundsson *et al.*, 2015). Available time at onset of supraglacial flow was estimated using the assumption that all the meltwater is released instantaneously ($t_{Q_{max}} = 0$). As a consequence, $SpTT_{Q_{max}}$ was considered the equivalent of $SpTT_{min}$.

Results of the calculations indicate that the national road is cut by floodwater within a minimum of 13 minutes by Hnappavellir, on the southern slopes of Örfafajökull Volcano (Suðurhlíðar) (Figure VII-13, Figure VII-14), and 26 minutes by Freysnes, at the foot of Svínafellsjökull Glacier (Figure VII-13, Figure VII-15).

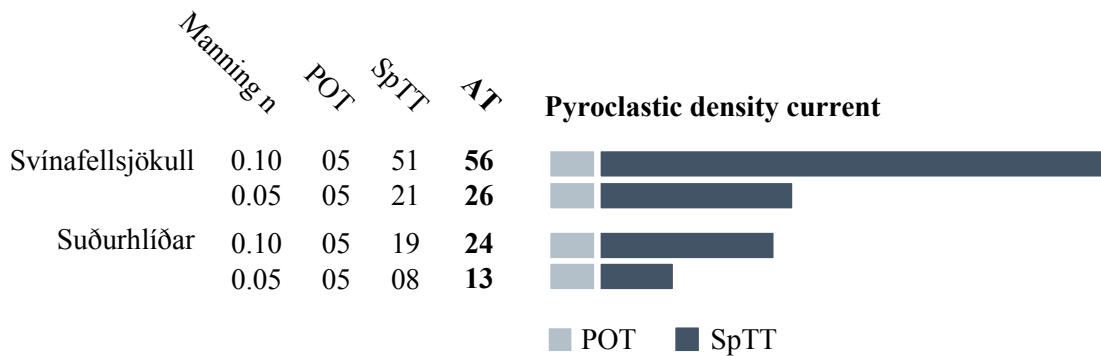


Figure VII-13: Available time at onset of a pyroclastic density current (AT_{pdc}) before floodwater reaches the National road. $AT_{pdc} = POT_{min} + SpTT_{min}$, where POT_{min} is the estimated PDC onset time (Gudmundsson *et al.*, 2015) and $SpTT_{min}$ the minimum flood travel times at the glacier surface and on proglacial terrains for Manning n roughness coefficients 0.05 and 0.10 (Helgadóttir *et al.*, 2015).

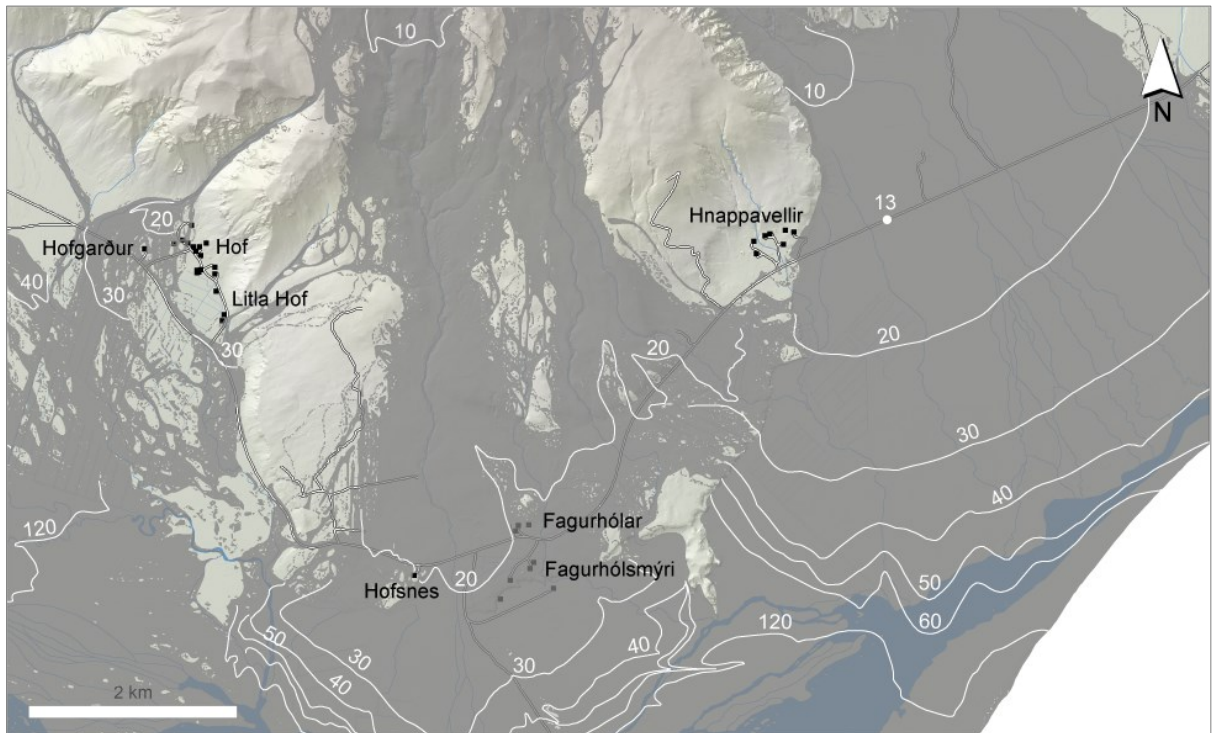


Figure VII-14: Minimum time available for evacuation (10-min isochrones) should a pyroclastic flow density current cause a flood on the southern slopes of Örfajökull Volcano. Maximum discharge attained at onset of supraglacial flow ($t_{Q_{max}} = 0$) is used as an assumption. Inundation extent in the proglacial area is shown as a grey overlay.

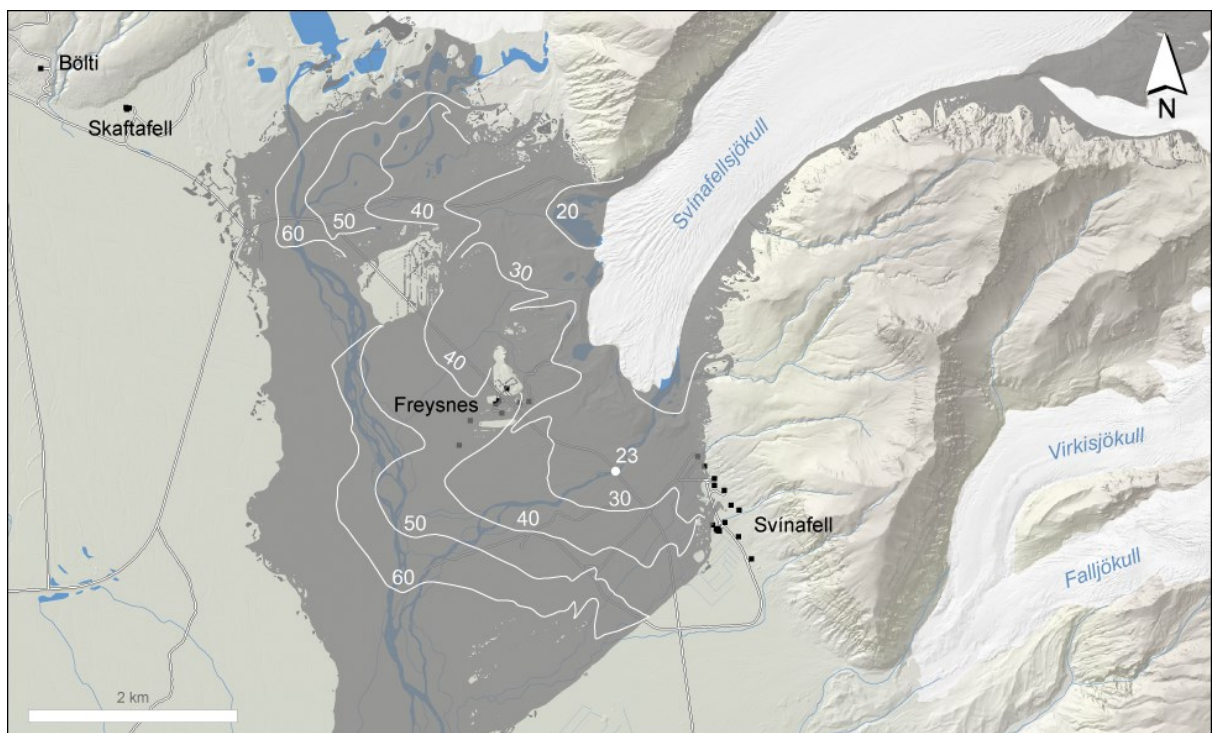


Figure VII-15: Minimum time available for evacuation (10-min isochrones) should a pyroclastic flow density current cause a flood on the slopes of Svínafellsjökull Glacier. Maximum discharge attained at onset of supraglacial flow ($t_{Q_{max}} = 0$) is used as an assumption. Inundation extent in the proglacial area is shown as a grey overlay.

3. Time required for evacuation

The notions of required safe exit time (RSET) and total evacuation time (TET) were used as expressions of the time required for evacuation. Devised by the community of fire safety engineers for timeline modelling of building evacuation (Pauls, 1980), the two notions are also used in the modelling of flood evacuation.

RSET refers in this study to the minimum time required, from departure nodes to fixed exits points placed on the National road

(Table VII-3, Figure VII-16), for evacuating the proglacial terrains facing the Örfajökull glacier catchments, including areas identified at risk of flooding in the numerical simulations performed by Helgadóttir *et al.* (2015) and adjacent terrains. The departure nodes considered in the analysis correspond to residences, accommodations premises, and the main visiting sites whose access points on the National road are located within the exit points. Although having one of its access points safely accessible in the eventuality of floods caused by an eruption of Örfajökull Volcano, Skaftafell was included in the analysis for informative purpose.

Table VII-3: Exit points used for RSET and TET computations.

Exit points	General location	Latitude	Longitude
W1	Skaftafell	63,99064	-16,95626
E1	Kvísker	63,97284	-16,42029
E2	Jökulsárlón	64,04605	-16,17743

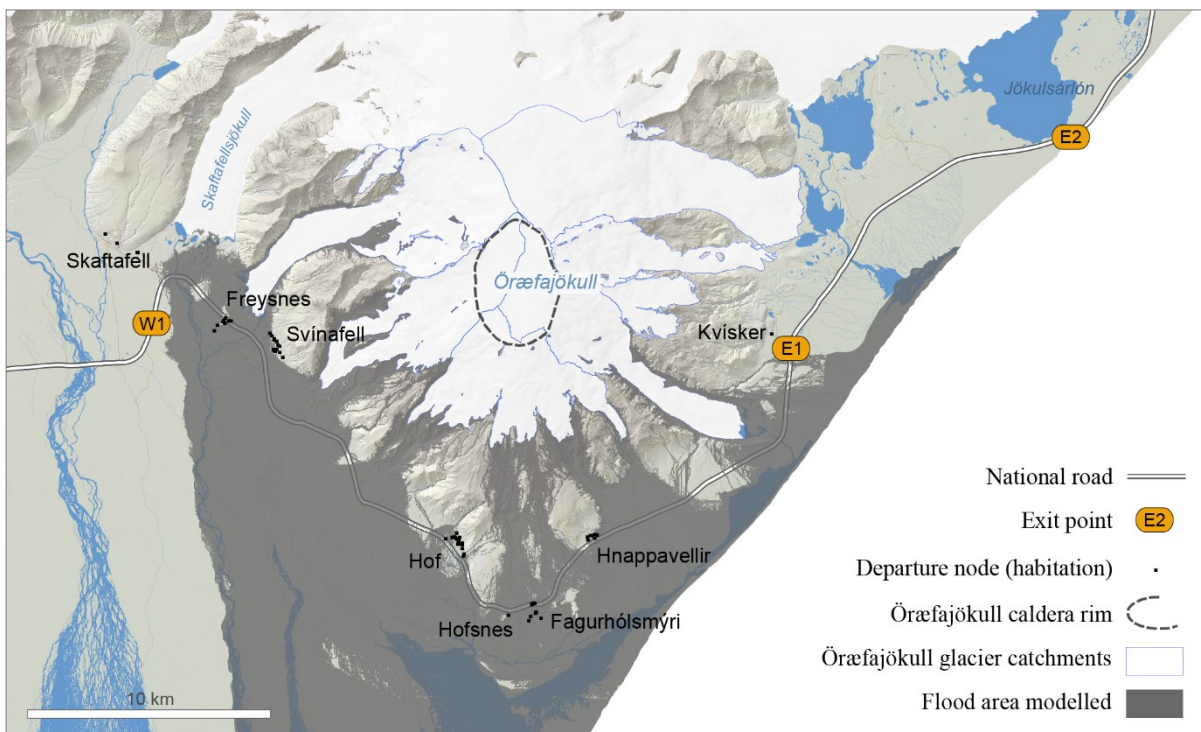


Figure VII-16: Exit points used in the estimation of required safe exit time, using the National road as a way out. Extent of the flood area is after Helgadóttir *et al.* (2015).

From each departure node, RSET was quantified as following:

$$RSET = RT + WT + TT$$

where RT is the response time before departure, WT the waiting time after the first element of the vehicle queue has left until the last element of the queue moves on, and TT the average travel time to exits points.

TET refers in this study to the minimum time necessary for the complete evacuation of the areas found within the exit points and should be regarded in this regard as equalling the highest of the RSET values:

$$TET = \max \{RSET_1, \dots, RSET_n\}$$

3.1. Response time before departure

Response time before departure represents in this study the time effectively spent before evacuees are ready to leave. It does include the duration of the recognition phase, i.e. the time necessary for understanding the necessity of evacuating, also termed warning acceptance factor and characterised by response inertia (Opper *et al.*, 2010), and the time effectively needed for preparation upon acceptance.

Duration of the recognition phase is likely to vary between residents and tourists, as these two populations often show different levels of awareness and knowledge of the ongoing and forthcoming events (Bird *et al.*, 2010).

For convenience, response time before departure was fixed to a 15-minute average.

3.2. Waiting time at departure

Waiting time, which is defined as the time elapsed, at departure nodes, after the first element of the vehicle queue has left until the last element of the queue moves on, was quantified using travel demand estimates and a time interval between each vehicle of the queue.

The time interval between each vehicle of the queue was fixed to a minimum of three seconds, which correspond, in optimal weather conditions, to the rounded up safe following time between vehicles (Knipling *et al.*, 1993). Travel demand was determined as the number of vehicles available for evacuation at each departure node, using estimations on the number of evacuees therefrom and estimates on the number of evacuees per vehicle.

3.2.1. Number of evacuees

Night-time exposure estimates proposed by Pagneux (2015) were used to quantify the minimum and maximum number of evacuees — residents or transients (all non-residents, such as tourists and seasonal workers, etc.) — at each departure node. Minimum figures correspond to the winter visiting respite, when residents form the main body of evacuees, while maxima correspond to the summer seasonal peak, when tourists represent a factor-9 increase of the local population (Pagneux, 2015).

3.2.2. Passengers per vehicle

There is little information available to support an estimation of the likely number of passengers per vehicle. Road traffic survey made in Berufjörður during the summer 2008 (Brynjarsson, 2009) suggests an average of 2 passengers per vehicle, without further discrimination between individual cars and passenger vehicles of a capacity >9 individuals.

In the present case, averages of 2–3 passengers for individual cars and 20–25 passengers for buses were used (Table VII-4). For each departure node, deciding on the number of passengers per vehicle was based on whether evacuees are residents or transients, and whether accommodation premises at which transients can be found offer enough beds to host groups travelling by bus.

Table VII-4: Number of passenger per vehicle, based on the type of population and of accommodation premise.

Population	Beds	car	bus
Residents		2–3	-
Accommodation premises	No group capacity	2–3	-
Accommodation premises	Group capacity	2–3	20–25

3.2.3. Computed travel demand

A maximum travel demand ranging 230–335 vehicles was found at departure nodes having access to the National road between the exit points W1 and E2 (Table VII-5). At locations where the contingent of evacuees is dominated by transients, the maximum demand was estimated to be oscillating

between 25–40 vehicles (Svínafell) and 125–185 vehicles (Skaftafell). A maximum demand < 5 vehicles was found at locations where the contingent of evacuees is only made of residents.

3.2.4. Waiting time estimates

Analysing together the travel demand estimates and the time interval between vehicles (three seconds) gave a maximum waiting time < 1 minute at locations where the contingent of evacuees is only made of residents (Table VII-6). At nodes where the contingent of evacuees is dominated by non-residents (Skaftafell, Freysnes, Hof, Svína-fell), minimum waiting time was estimated <2 minutes and maximum waiting time ranging 2–9 minutes.

Table VII-5: Maximum travel demand (number of vehicles) at departure nodes, based on night-time exposure figures from Pagneux (2015) and passenger-per-vehicle estimates. The share of evacuation by bus and by individual car is highly tentative.

Departure node	Transients, as maximum share of overall population			maximum travel demand (number of vehicles)
	All (%)	thereof by bus (%)	thereof by car (%)	
Skaftafell, Bölti	99.6	20	80	125 – 185
Freysnes	80.5	49	51	25 – 45
Svínafell	82	25	75	25 – 40
Hof, Litla Hof	84	17	83	40 – 55
Hofsnes	0	-	-	< 5
Fagurhólsmýri, Fagurhólar	0	-	-	< 5
Hnappavellir	0	-	-	< 5
Kvísker	0	-	-	< 5
Total				230 – 335

Table VII-6: Waiting time at departure nodes based on minimum/maximum travel demand and minimum time interval between vehicles (Safe following distance). Time values are rounded to the highest integer.

Departure node	Time interval between vehicles (seconds)	Travel demand		Waiting time (min.)	
		min	max	min	max
Skaftafell, Bölti	3	< 5	185	1	9
Freysnes	3	< 10	45	1	2
Svínafell	3	< 10	40	1	2
Hof, Litla-Hof	3	< 10	55	1	3
Hofsnes	3	< 5	< 5	1	1
Fagurhólsmýri, Fagurhólar	3	< 5	< 5	1	1
Hnappavellir	3	< 5	< 5	1	1
Kvísker	3	< 5	< 5	1	1

3.3. Average travel time to exit points

Average travel times between departure nodes and exit points were determined as the sum of average running times on road segments in optimal weather conditions and stopping times at network access points (Fitzpatrick *et al.*, 2003).

Every road segment was attributed an average running time, defined as the length of the segment considered divided by the average running speed at which a normalised vehicle traverses the segment. A normalised vehicle is defined here as every motorised vehicle — car, bus, or motorcycle — capable of reaching at least the highest mandatory or posted speed limits. Running time refers to the time a normalised vehicle spend in motion, and was estimated in this study using fixed average running speeds (Table VII-7) obtained from a combined analysis of available information on regulatory or posted speed limits (IRCA, 2010) and types of roads, including type of surface, terrain, road curvatures, segment lengths, lane widths, and bottlenecks dimensions. Stopping times, i.e. the time spent on stopping at access points and bottlenecks, was taken into account by applying a 10-percent pejoration to the average running times.

3.3.1. Types of roads

Three types of roads, either public or private, are found in the study area: C, D, and F (NLSI, 2012). Type C corresponds to double-lane roads ranging 6.5–10 metres in width, type D corresponds to single-lane roads with shoulders and types F1, F2, and F3 corresponds to mountain roads (IRCA, 2014). Surface of types C and D, which are developed on fills and are found on flat terrains, is of asphalt or compacted gravel. Mountain roads are found on flat or hilly terrains and usually entail the land surface.

3.3.2. Bottlenecks

No less than 20 bridges are present on the 85 km of the National road's stretch laying between Lómagnúpur to the west and Jökulsárlón proglacial Lagoon to the east. Half of them are single-lane structures measuring 3.2–4.2 in width, the longest of them, on the Skeiðará river, measuring 880 m (IRCA, 2011; Figure VII-17).

The seven single-lane bridges located in the area identified at risk of flooding should an eruption of Öräfajökull volcano happen (Helgadóttir *et al.*, 2015) are not long enough to impact significantly on running speeds and travel times. In turn, any accident on the Skeiðará Bridge has the potential to interrupt totally road traffic as exemplified by the June 26 2013 event, when the bridge was closed

for more than one hour as a vehicle was stuck on the lane. Two other accidents, in 2004 and 2011, led to close the bridge temporarily. As the bridge is only 4.4 km away from the flood hazard zone identified by Helgadóttir *et al.* (2015), any closure would hinder, in the west direction, evacuation of the areas exposed to volcanogenic floods. Disuse of the Skeiðará Bridge has been planned by the Icelandic

Road and Coastal Administration and will become effective upon completion, upstream, of a 70 m long double-lane bridge expected to open to traffic in the fall 2016 (Rögnvaldur Gunnarsson, personal communication). Any evacuation of the Öraefi district will certainly benefit from these improvements to the road local infrastructure.

Table VII-7: Average running speeds estimation (range) for road types C, D, and F.

Type	Description	Average running speed (range, in km/h)	Surface	Terrain
C	Double-lane road $6.5 \leq \text{full width} \leq 10 \text{ m}$	10 – 90	Asphalt or gravel	Flat
D	Single-lane road with shoulders	10 – 80		
F1	Mountain road	10 – 30	Earth	Flat or hilly
F2	Mountain road	10 – 20		
F3	Mountain road	10		



Figure VII-17: Single-lane bridges (red-filled circles) located on the Lómagnúpur - Jökulsárlón National road's segment (Source: IRCA, 2011). Seven bridges are located in the area identified at risk of volcanogenic floods (grey area) by Helgadóttir *et al.* (2015).

3.3.3. Computed travel times

Results of the calculations suggest that in optimal weather conditions, running times should not exceed 27 minutes on the segment W1-E1 and 37 minutes on the segment W1-E2 (Table VII-3, Table VII-8).

With the exception of Bölti and Skaftafell, all the departure nodes were found within a one-minute drive from the National road. Considering together average running times and stopping times, it was found that reaching exit point W1 should not require more than a 20-minute drive (Table VII-9). Average travel times from departure nodes to exits point E1 (Skaftafell and Kvísker excluded) and E2 (Skaftafell excluded) ranged 10–27 minutes and 21–38 minutes respectively.

3.4. Total evacuation time

Based on the sum of response time, waiting time and travel times, it appears that in optimal weather conditions, the area enclosed between exit points W1 and E1 is unlikely to be fully evacuated in less ~30 minutes (Table VII-10). A full evacuation of the area enclosed between exit points W1 and E2 should not take less than ~35 minutes.

The situation is much different from one departure node to the other. Required safe exit time was estimated to a minimum of 20 minutes from Freysnes to the nearest exit point, 32 minutes from Hof and 29 minutes from Hofsnæs (Table VII-10). Similarly, evacuation from Hnappavellir to exit point E1 would take a minimum of 29 minutes, extended to 36 minutes should evacuees be required to reach exit points E2 or W1.

Table VII-8: Segments lengths, average running speeds and average running times between exits points. Values are rounded to the nearest integer.

Road segment	Segment length (km)	Average running speed (km/h)	Average running times (min.)
W1 – E1	39	88	27
E1 – E2	15	89	10
W1 – E2	54	89	37

Table VII-9: Average travel times (min.) from departure nodes to exits points W1, E1, and E2. Values are rounded to the nearest integer.

Departure node	W1	E1	E2
Skaftafell, Bölti	7	-	-
Freysnes	3	27	38
Svínafell	5	26	38
Hof, Litla-Hof	14	17	29
Hofsnæs	16	14	25
Fagurhólsmýri, Fagurhólar	18	13	25
Hnappavellir	20	10	21
Kvísker	-	-	11

Table VII-10: Required safe exit times (min.), in optimal weather conditions, from departure nodes to exit points W1, E1 and E2. Values are rounded to the nearest integer.

Departure node	Exit point W1		Exit point E1		Exit point E2	
	Min	Max	Min	Max	Min	Max
Skaftafell, Bölti	24	32	-	-	-	-
Freysnes	19	20	43	44	53	54
Svínafell	21	22	42	43	53	54
Hof, Litla-Hof	30	32	33	35	44	45
Hofsnes	32	32	29	29	39	39
Fagurhólsmýri, Fagurhólar	33	33	29	29	39	39
Hnappavellir	36	36	26	26	36	36
Kvísker	47	47	-	-	27	27

As an optimal time interval of three seconds between vehicles was used (Table VII-6), seasonal changes in travel demand were found of little impact on evacuation time (Table VII-10). Any change to worse weather conditions could lead not only to a reduction of average running time but also to an increase of the safe following distance, giving incidentally more weight to seasonal patterns in travel demand. For instance, increasing the time interval between vehicles to six seconds — the recommended safe following interval in rainy conditions — would lead to a 10-minute increase for completing evacuation of Skaftafell during the summer peak.

A detailed assessment of the spatial distribution of residents and transients during daytime, comparable to what was made in Pagneux (2015) for night time exposure, is not available at present. Experience suggests that during the visiting season, the vast majority of the population can be found by day on and around the two sites of Skaftafell and Jökulsárlón, which are both located beyond the flood risk area identified in Helgadóttir *et al.* (2015). On that basis, it is reasonable to think that the population located in the areas at risk of flooding is not as important during daytime as it is during night-time. It is unlikely, however, to find at any hour of the day a departure node empty of evacuees.

4. Evacuation routes

Estimates on required safe exit times (see §2) were used to determine the shortest routes evacuees should follow, from departure nodes to the nearest exit point on road segments W1-E1 and W1-E2. The National road was divided in two routes, here referred to as the “western” and “eastern” routes.

4.1. Road segment W1-E1

Evacuees from Hof, Svínafell, and Freysnes would be required to drive west to exit point W1 (Table VII-11, Figure VII-18). E1 would be in turn the nearest exit point for evacuees located in Hofsnes, Fagurhólsmýri, and Hnappavellir. The evacuation route divide is located between the Hof and Hofsnes settlements (Figure VII-18).

4.2. Road segment W1-E2

Evacuees from Fagurhólsmýri, Hofsnes, Hof, Svínafell, and Freysnes would be required to drive west to exit point W1 (Table VII-12, Figure VII-19). E2 would be the nearest for evacuees located at Kvísker. As the evacuation route divide is located by Hnappavellir, evacuees therefrom could equally drive east or west.

Table VII-11: Required safe exit time (RSET) from departure nodes to nearest exit point on road segment W1-E1.

Departure node	Nearest exit point	RSET (min.)
Freysnes	W1	19 – 20
Svínafell	W1	21 – 22
Hof, Litla Hof	W1	30 – 32
Hofsnes	E1	29
Fagurhólmýri, Fagurhólar	E1	29
Hnappavellir	E1	26

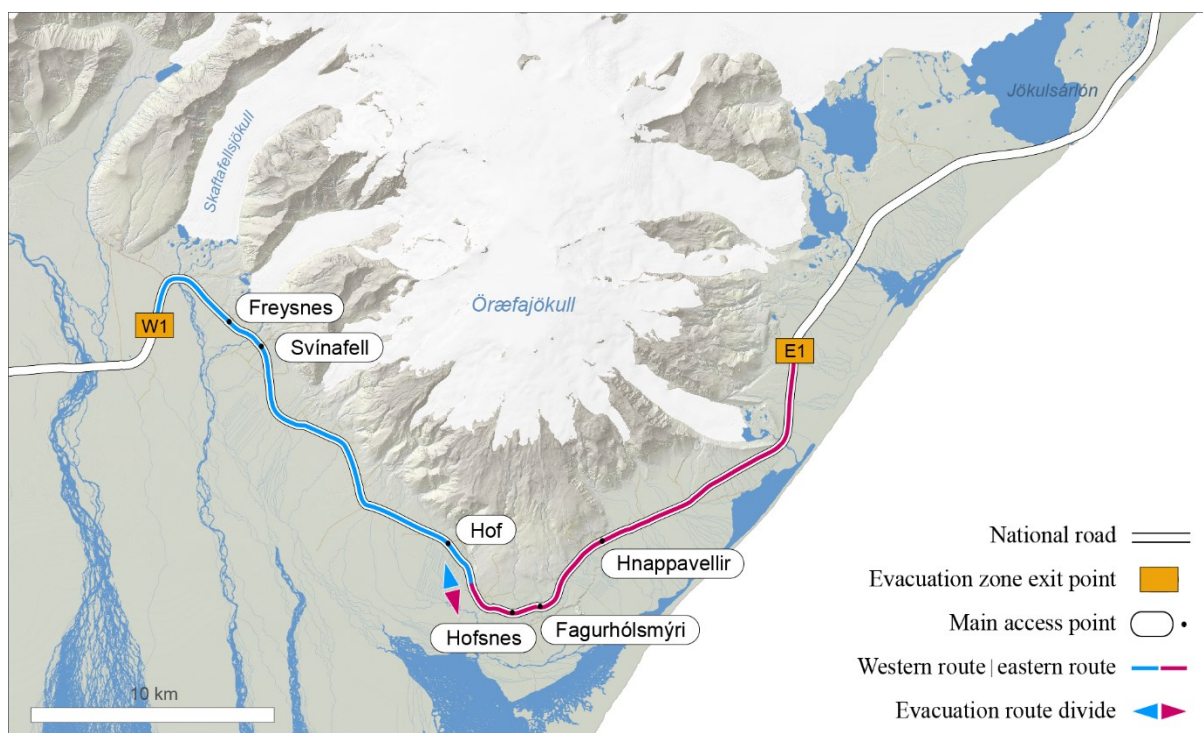


Figure VII-18: Routing of evacuation between W1 and E1 exit points.

Table VII-12: Required safe exit time (RSET) from departure nodes to nearest exit point on road segment W1-E2.

Departure node	Nearest exit point	RSET (min.)
Freysnes	W1	19 – 20
Svínafell	W1	21 – 22
Hof, Litla Hof	W1	30 – 32
Hofsnes	W1	32
Fagurhólmýri, Fagurhólar	W1	33
Hnappavellir	W1, E2	36
Kvísker	E2	27

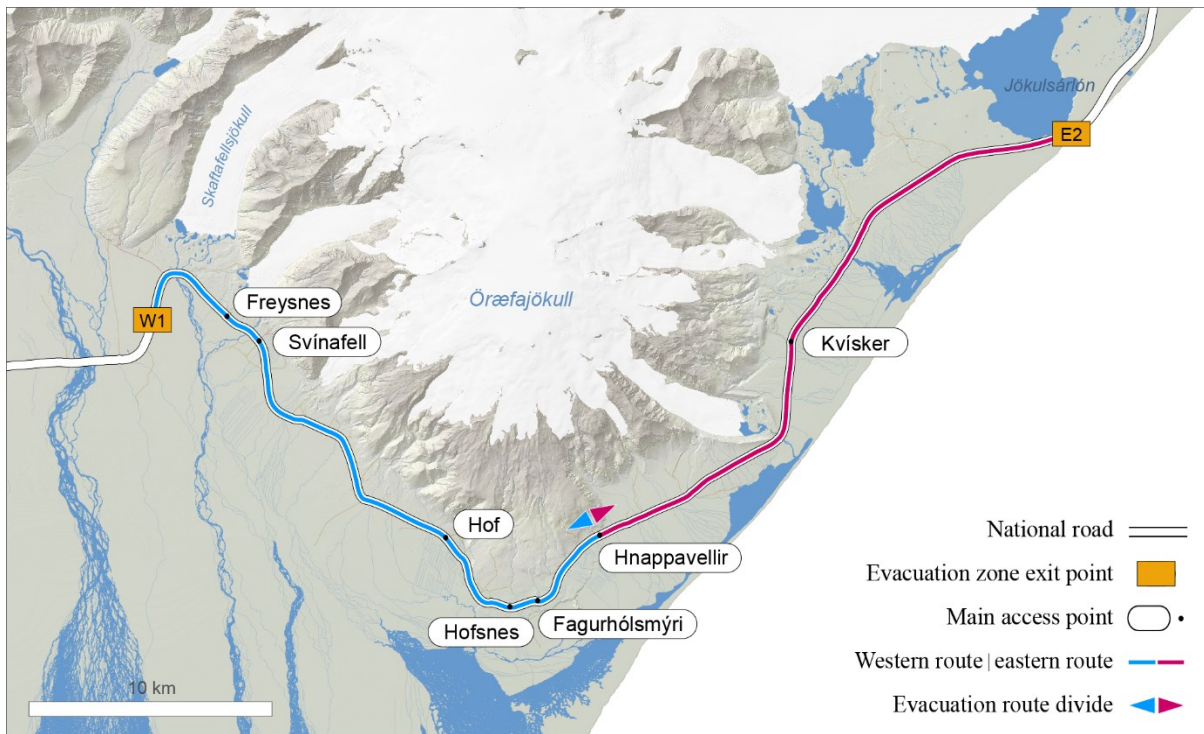


Figure VII-19: Routing of evacuation between W1 and E2 exit points.

5. Shelters

The results indicate that the time required exceeds, at eruption onset, the time actually available for a full evacuation of the areas at risk of flooding. Therefore, achieving partial or full evacuation of these areas before eruption onset may be regarded as a desirable objective. It corresponds, however, to an ideal situation where information necessary to order and secure evacuation ahead of an eruption is at hand. A situation where evacuation does not take place before an eruption starts cannot be excluded and, therefore, the possibility of sheltering in place the population that cannot evacuate in time should be considered by the authorities. Such a possibility is not investigated in this study.

6. Summary and conclusion

The time available and the time required for evacuating areas exposed to floods caused by eruptive activity of Öraefajökull Volcano was assessed, and evacuation routes determined.

Estimations on time availability were made at onset of a volcanic eruption initiated in the

caldera or on the flanks of the volcano, and at onset of pyroclastic density currents. The melting scenarios elaborated by Gudmundsson *et al.* (2015), and the results of the numerical simulations performed accordingly by Helgadóttir *et al.* (2015) were used to this end. Estimation of the time required for the evacuation was quantified as the sum of response time before departure, waiting time at departure nodes, and average travel times from departure nodes to fixed exits points marking the boundaries of areas to be evacuated. Night-time exposure estimates proposed by Pagneux (2015) were used to quantify the minimum and maximum number of evacuees — residents or guests — at each departure node.

Results of the modelling suggest that areas at risk of flooding are unlikely to be successfully evacuated once an eruption has started. It was found that the National road — the only terrestrial axis of evacuation existing at present, could be flooded at multiple locations within the range of 20–30 minutes at onset of a volcanic eruption in the caldera or on the flanks (Figure VII-9 to Figure VII-12), and within 15–25 minutes at onset of a

pyroclastic density current (Figure VII-13 to Figure VII-15). In the meantime, it was found that in optimal weather conditions, a full evacuation could not be achieved in less than 30–35 minutes (Table VII-10).

As the time required for a full evacuation of the areas at risk of flooding exceeds, at eruption onset, the time actually available for the evacuation, it is crucial to rely on early precursors of volcanic activity and have the areas evacuated before eruption start. As the possibility of an eruption starting before any evacuation is initiated cannot be excluded, the feasibility of sheltering in place the populations that cannot evacuate timely should also be considered. This has to be thought of carefully, as sheltered people may no longer have the possibility to escape the district after the floods, and therefore be severely exposed to the other primary volcanic hazards that will certainly follow, such as tephra fall and lightning.

7. Acknowledgements

The author would like to thank Ágúst Gunnar Gylfason and Magnús Tumi Gudmundsson for their support during the framing of this work. Ásdís Helgadóttir, Haraldur Sigþórsson and Tómas Jóhannesson are thanked for their review and proof-reading of the chapter.

The present work was funded by the Icelandic Avalanche and Landslide Fund, the National Power Company, and the Icelandic Road and Coastal Administration.

8. References

- Bird, D. K., Gísladóttir, G., & Dominey-Hoves, D. (2010). Volcanic risk and tourism in southern Iceland: Implications for hazard, risk and emergency response education and training. *Journal of Volcanology and Geothermal Research*, 189, 33–48.
- Brynjarsson, F. (2009). *Berufjörður. Umferðarkönnun 17. og 19. júlí 2008 (Berufjörður: July 17–19 2008 traffic survey)*. Icelandic Road and Coastal Administration. Reykjavík: Icelandic Road and Coastal Administration.
- Fitzpatrick, K., Carlson, P., Brewer, M., & Wooldridge, M. D. (2003). *Design speed, operating speed, and posted speed practices*. Washington D.C.: Transportation Research Board of the National Academies.
- Gudmundsson, M. T., Högnadóttir, Þ., & Magnússon, E. (2015). Öraefajökull: Eruption melting scenarios. In E. Pagneux, M. T. Gudmundsson, S. Karlsdóttir, & M. J. Roberts (Eds.), *Volcanogenic floods in Iceland: An assessment of hazards and risks at Öraefajökull and on the Markarfljót outwash plain* (pp. 45–72). Reykjavík: IMO, IES-UI, NCIP-DCPEM.
- Gudmundsson, M. T., Larsen, G., Höskuldsson, Á., & Gylfason, Á. G. (2008). Volcanic hazards in Iceland. *Jökull*, 58, 251–258.
- Helgadóttir, Á., Pagneux, E., Roberts, M. J., Jensen, E. H., & Gíslason, E. (2015). Öraefajökull Volcano: Numerical simulations of eruption-induced jökulhlaups using the SAMOS flow model. In E. Pagneux, M. T. Gudmundsson, S. Karlsdóttir, & M. J. Roberts (Eds.), *Volcanogenic floods in Iceland: An assessment of hazards and risks at Öraefajökull and on the Markarfljót outwash plain* (pp. 75–102). Reykjavík: IMO, IES-UI, NCIP-DCPEM.
- IRCA (2010). *Þjóðvegir í þéttbýli. Leiðbeiningar 2010 (National roads intersecting urban areas. Guidelines 2010)*. Icelandic Road and Coastal Administration.
- IRCA (2011). *Brúaskrá. Bryr á þjóðvegum (Bridge Register. Bridges on the National road)*. Retrieved 5 5, 2014, from [http://www.vegagerdin.is/Vefur2.nsf/Files/Bruaskra-a-thjodv/\\$file/Bruaskra-a-tjodvegum.pdf](http://www.vegagerdin.is/Vefur2.nsf/Files/Bruaskra-a-thjodv/$file/Bruaskra-a-tjodvegum.pdf)
- IRCA (2014). *Vegtegundir (Road types)*. Retrieved 5 5, 2014, from <http://www.vegagerdin.is/vegakerfid/vegtegundir>
- Knipling, R., Mironer, M., Hendricks, D., Tijerina, L., Everson, J., Allen, J., & Wilson, C. (1993). *Assessment of IVHS countermeasures for collision avoidance*. US Department of Transportation. Washington: National Highway Traffic Safety Administration.
- Mileti, D., Bolton, P., Fernandez, G., & Updike, R. (1991). *The eruption of Nevado del Ruiz Volcano Colombia, South America, November 13, 1985*. (Commission on Engineering and Technical Systems, Ed.) Washington D.C.: National Academy Press.
- NLSI (2012). IS 50V Geodatabase. (version 3.4). National Land Survey of Iceland.
- Opper, S., Cinque, P., & Davies, B. (2010). Timeline modelling of flood evacuation operations. *Procedia Engineering*, 3, 175–187.

- Pagneux, E. (2015). Öräfi district and Markarfljót outwash plain: Spatio-temporal patterns in population exposure to volcanogenic floods. In E. Pagneux, M. T. Gudmundsson, S. Karlsdóttir, & M. J. Roberts (Eds.), *Volcanogenic floods in Iceland: An assessment of hazards and risks at Öräfajökull and on the Markarfljót outwash plain* (pp. 123–140). Reykjavík: IMO, IES-UI, NCIP-DCPEM.
- Pagneux, E., & Roberts, M. J. (2015). Öräfi district and Markarfljót outwash plain: Rating of flood hazards. In E. Pagneux, M. T. Gudmundsson, S. Karlsdóttir, & M. J. Roberts (Eds.), *Volcanogenic floods in Iceland: An assessment of hazards and risks at Öräfajökull and on the Markarfljót outwash plain* (pp. 101–122). Reykjavík: IMO, IES-UI, NCIP-DCPEM.
- Pauls, J. (1980). Building evacuation: research findings and recommendations. In D. V. Canter (Ed.), *Fires and human behaviour* (pp. 251–276). Chichester: J. Wiley.
- Roberts, M. J., & Gudmundsson, M. T. (2015). Öräfajökull Volcano: Geology and historical floods. In E. Pagneux, M. T. Gudmundsson, S. Karlsdóttir, & M. J. Roberts (Eds.), *Volcanogenic floods in Iceland: An assessment of hazards and risks at Öräfajökull and on the Markarfljót outwash plain* (pp. 17–44). Reykjavík: IMO, IES-UI, NCIP-DCPEM.
- Thorarinsson, S. (1958). The Öräfajökull eruption of 1362. *Acta Naturalia Islandica*, 2(4), 100.
- Vogfjörð, K. S., Jakobsdóttir, S. S., Gudmundsson, G. B., Roberts, M. J., Ágústsson, K., Arason, T., Geirsson, H., Karlsdóttir, S., Hjaltadóttir, S., Ólafsdóttir, U., Thorbjarnardóttir, B., Hafsteinson, G., Sveinbjörnsson, H., Stefánsson, R., and Jónsson, T. V. (2005). Forecasting and monitoring a subglacial eruption in Iceland. *EOS*, 86(26), 245–248.
- Voigt, B. (1990). The 1985 Nevado del Ruiz volcano catastrophe: anatomy and retrospection. *Journal of Volcanology and Geothermal Research*, 44, 349–386.
- Zobin, V. M. (2011). *Introduction to Volcanic Seismology* (2nd ed.). Amsterdam: Elsevier Science.

